



On the two-pole nature of the $\Lambda(1405)$ from Lattice QCD

EMMI Workshop and International Workshop L on Gross
Properties of Nuclei and Nuclear Excitations:
“Strong interaction physics of heavy flavors”

Bárbara Cid-Mora

January 18th, 2024

HIM

HELMHOLTZ

Helmholtz-Institut Mainz



TECHNISCHE
UNIVERSITÄT
DARMSTADT

HGS-HIRe for FAIR

Helmholtz Graduate School for Hadron and Ion Research



Lattice QCD study of $\pi\Sigma-\bar{K}N$ scattering and the $\Lambda(1405)$ resonance

John Bulava,¹ Bárbara Cid-Mora,² Andrew D. Hanlon,³ Ben Hörz,⁴ Daniel Mohler,^{5,2} Colin Morningstar,⁶
Joseph Moscoso,⁷ Amy Nicholson,⁷ Fernando Romero-López,⁸ Sarah Skinner,⁶ and André Walker-Loud⁹
(for the Baryon Scattering (BaSc) Collaboration)

A lattice QCD computation of the coupled channel region is detailed. Results are obtained using a $2+1$ dynamical quark flavors and $m_\pi \approx 200$ MeV total momenta and irreducible representations are scattering K -matrix are utilized to obtain the K -matrix. The amplitudes, continued to the complex energy threshold and a resonance pole just below the \bar{K}

The two-pole nature of the $\Lambda(1405)$ from lattice QCD

John Bulava,¹ Bárbara Cid-Mora,² Andrew D. Hanlon,³ Ben Hörz,⁴ Daniel Mohler,^{5,2} Colin Morningstar,⁶
Joseph Moscoso,⁷ Amy Nicholson,⁷ Fernando Romero-López,⁸ Sarah Skinner,⁶ and André Walker-Loud⁹
(for the Baryon Scattering (BaSc) Collaboration)

This letter presents the first lattice QCD computation of the coupled channel $\pi\Sigma-\bar{K}N$ scattering amplitudes at energies near 1405 MeV. These amplitudes contain the resonance $\Lambda(1405)$ with strangeness $S = -1$ and isospin, spin, and parity quantum numbers $I(J^P) = 0(1/2^-)$. However, whether there is a single resonance or two nearby resonance poles in this region is controversial theoretically and experimentally. Using single-baryon and meson-baryon operators to extract the finite-volume stationary-state energies to obtain the scattering amplitudes at slightly unphysical quark masses corresponding to $m_\pi \approx 200$ MeV and $m_K \approx 487$ MeV, this study finds the amplitudes exhibit a virtual bound state below the $\pi\Sigma$ threshold in addition to the established resonance pole just below the $\bar{K}N$ threshold. Several parametrizations of the two-channel K -matrix are employed to fit the lattice QCD results, all of which support the two-pole picture suggested by $SU(3)$ chiral symmetry and unitarity.

The two-pole nature of the $\Lambda(1405)$ from Lattice QCD *

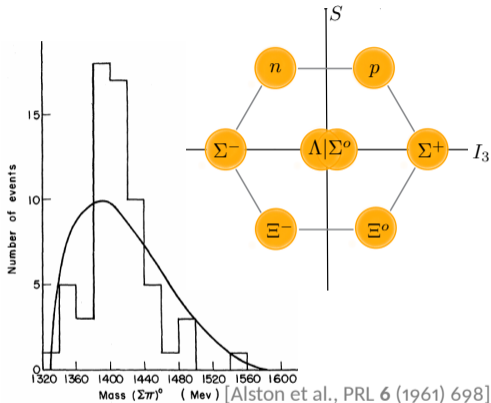
Lattice QCD study of $\pi\Sigma - \bar{K}N$ scattering and the $\Lambda(1405)$ resonance **

* Letter (Accepted by PRL): 2307.10413

** Long paper (Accepted by PRD): 2307.13471

Table of Contents

- ⦿ About the $\Lambda(1405)$
- ⦿ Lattice QCD
- ⦿ Finite-volume energy spectra
- ⦿ Scattering amplitude analysis
- ⦿ Summary



$$\Lambda(1405) \rightarrow I(J^P) = 0\left(\frac{1}{2}^-\right) \quad S = -1$$

- Theoretical Prediction $K^- p \rightarrow \pi \Sigma$
[Dalitz & Tuan, PRL 2 (1959) 425]
- Experimental evidence of resonance ($\pi \Sigma$ mass spectrum)
[Alston et al., PRL 6 (1961) 698]
- Meson-Baryon comp. $\Lambda(1405)$ (Chiral sym.)
[Veit et al., PLB 137 (1984) 415]
[Jennings, PLB 176 (1986) 229]
- First time two-pole picture
[Fink et al., PRC 41 (1990) 2720]
- Chiral dynamics: coupled-channel
[Kaiser et al., NPA 594 (1995) 325]
[Oset & Ramos, NPA 635 (1997) 99]
- SIDDHARTA at DAΦNE: $K^- p$ Scattering Length det.
[Bazzi et al., PLB 704 (2011) 113]
- Spin & Parity by CLAS Collab.
[Moriya et al., PRC 87 (2013) 035206]
[Moriya et al., PRL 112 (2014) 082004]

Λ resonances

[PDG, PTEP **2022** (2022) 083C01]

Hadron	J^P	status
$\Lambda(1116)$	$1/2^+$	(* * *)
$\Lambda(1380)$	$1/2^-$	(**)
$\Lambda(1405)$	$1/2^-$	(* * *)
\vdots		

Is $\Lambda(1380)$ a second pole of the scattering amplitude in the complex energy plane in the $\Lambda(1405)$ region?

[Isgur & Karl, PRD **18** (1978) 4187]

[Oller & Meißner, PLB **500** (2001) 263]

[Roca & Oset, PRC **88** (2013) 055206]

[Mai & Meißner, EPJA **51** (2015) 30]

[Anisovich et al., EPJA **56** (2020) 139]

[Scheluchin et al., PLB **833** (2022) 137375]

[Wickramaarachchi et al., EPJ **271** (2022) 07005]

[Aikawa et al., PLB **837** (2023) 137637]

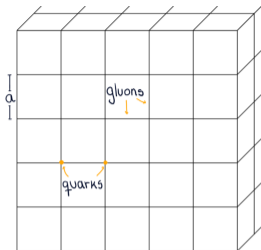
[Acharya et al., EPJC **83** (2023) 340]

* [Bulava et al., e-print: 2307.10413 (2023)]

* [Bulava et al., e-print: 2307.13471 (2023)]

Table of Contents

- ⦿ About the $\Lambda(1405)$
- ⦿ Lattice QCD
- ⦿ Finite-volume energy spectra
- ⦿ Scattering amplitude analysis
- ⦿ Summary



- Quarks and gluons in a finite size discretized grid
- Observables estimated by sampling gauge configurations
- Correlation functions are computed
- Finite-volume energy spectrum extraction

Importance of lattice QCD to study the $\Lambda(1405)$

→ Predictions once quark masses and couplings fixed

→ Facilitates exploration of the elastic region $\pi\Sigma - \bar{K}N$

→ Resulting motion of poles under variation of quark masses

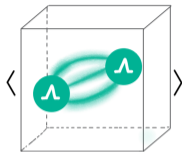
Details of the $D200$ ensemble generated by the Coordinated Lattice Simulations consortium (CLS):

[Bruno et al., JHEP 02 (2015) 043]

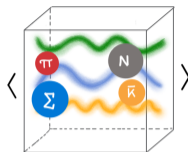
$a[fm]$	$(L/a)^3 \times (T/a)$	m_π	m_K	$m_\pi L$
0.0633(4)(6)	$64^3 \times 128$	≈ 200 MeV	≈ 487 MeV	4.181(16)

⊞ 2000 gauge configurations

⊞ Open temporal boundary conditions



Single hadron operator in the lattice (Λ)



Multihadron operators in the lattice ($\pi\Sigma$ and $\bar{K}N$)

► Operators

→ Single and two-hadron

- * $\Lambda[\vec{P}]$
- * $\pi[\vec{P}_1] \Sigma[\vec{P}_2]$
- * $\bar{K}[\vec{P}_1] N[\vec{P}_2]$

$\Lambda(\mathbf{d}^2)$	Operators
$G_{1g}(0)$	$\Lambda[G_{1g}(0)]_{0,1,3}$ $\bar{K}[A_2(1)]_1 N[G_1(1)]_0$ $\pi[A_2^-(1)]_1 \Sigma[G_1(1)]_0$

► **Correlation matrices** → Stochastic LapH method (sLaph)

[Peardon et al., PRD **80** (2009) 054506] (Original distillation)

[Morningstar et al., PRD **83** (2011) 114505]

$$C(t) = \langle \mathcal{O}_1(t) \bar{\mathcal{O}}_2(0) \rangle = \sum_n A_n e^{-tE_n}$$

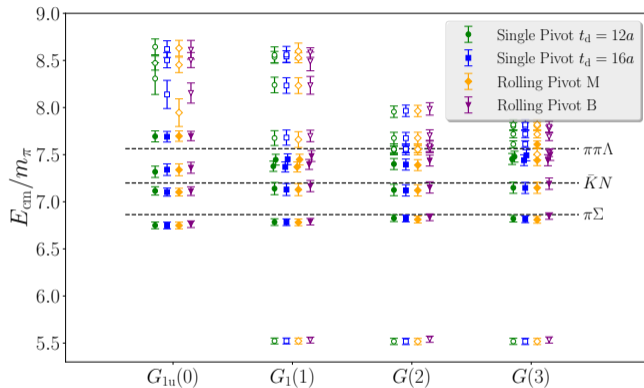
► **Extraction of energy spectra** → Solving the GEVP

[Michael & Teasdale, NPB **215** (1983) 433]

[Blossier et al., JHEP **04** (2009) 094]

$$C(t_d) \vec{v}_n(t_o, t_d) = \lambda_n(t_o, t_d) C(t_o) \vec{v}_n(t_o, t_d)$$

Single Pivot & Rolling Pivot



Center-of-mass finite-volume energy spectra results under variation of implementation of the GEVP method.

Table of Contents

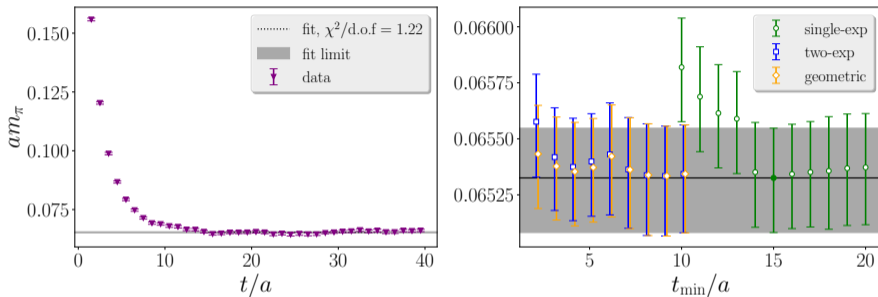
- ⦿ About the $\Lambda(1405)$
- ⦿ Lattice QCD
- ⦿ **Finite-volume energy spectra**
- ⦿ Scattering amplitude analysis
- ⦿ Summary

Several fit forms used to extract the finite-volume energy spectra:

$$C(t) = A_n e^{-tE_n} \text{ (Single exponential)}$$

$$C(t) = A_n e^{-tE_n} + A_1 e^{-tD^2} \text{ (Two-exponential)}$$

$$C(t) = \frac{A_n e^{-tE_n}}{1 - B e^{-Mt}} \text{ (Geometric)}$$



Single hadrons results: π effective mass and variety of fits to Lattice data using different values of t_{\min} .

Bulava et al., PRL (2023) [accepted] [arXiv:2307.10413]

Multihadron correlators treatment included

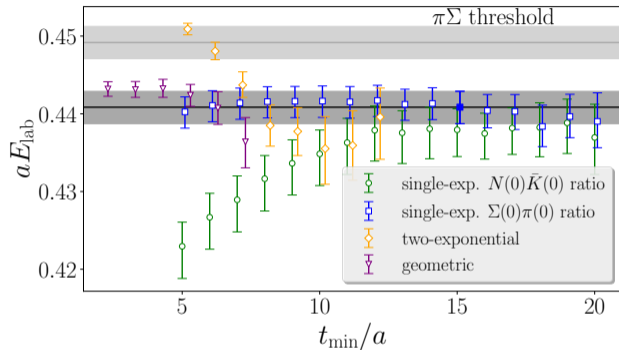
$$R_n(t) = \frac{D_n(t)}{C_A(\mathbf{d}_A^2, t)C_B(\mathbf{d}_B^2, t)} = A_n e^{-t\Delta E_n} \quad (\text{Ratio of correlators})$$

where aE_{lab} is reconstructed

$$aE_n^{\text{lab}} = a\Delta E + aE_n^{\text{non-int}}$$

and

$$E_n^{\text{non-int}} = \sqrt{m_A^2 + \left(\frac{2\pi\mathbf{d}_A^2}{L}\right)^2} + \sqrt{m_B^2 + \left(\frac{2\pi\mathbf{d}_B^2}{L}\right)^2}$$



Multihadron results: Variety of fit forms to lattice data vs t_{min} in the energy laboratory frame. (Lowest level of the $G_{1u}(0)$ irrep)

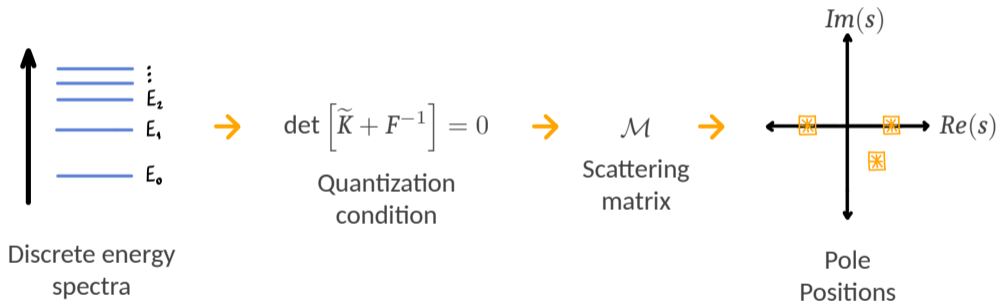
Bulava et al., PRL (2023) [accepted] [arXiv: 2307.13471]

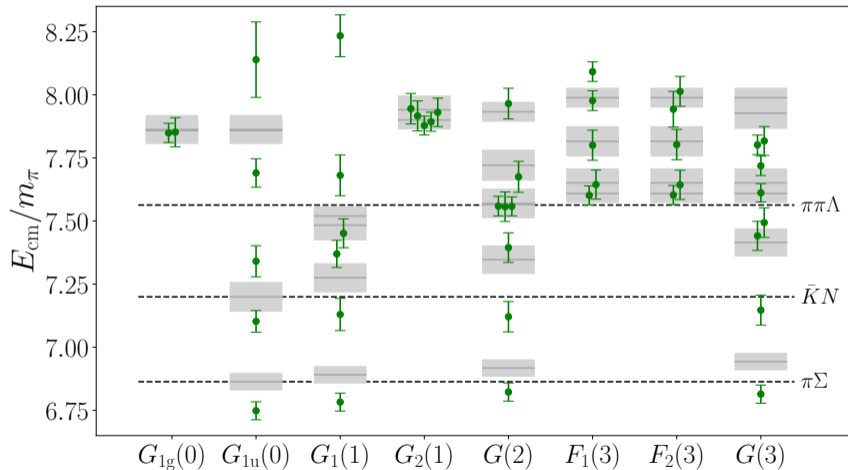
Table of Contents

- ⦿ About the $\Lambda(1405)$
- ⦿ Lattice QCD
- ⦿ Finite-volume energy spectra
- ⦿ Scattering amplitude analysis
- ⦿ Summary

The recipe for scattering amplitudes goes as

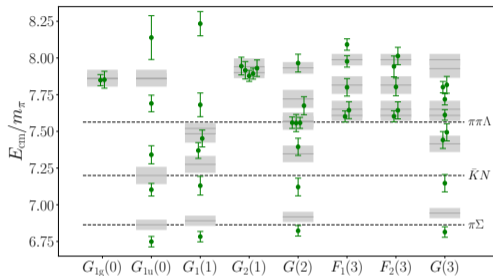
[M. Lüscher, NPB 354 (1991) 53] [M. Lüscher, NPB 364 (1991) 237; and extensions.]





Quantization condition

4 Scattering amplitude analysis



Finite-volume
energy spectra



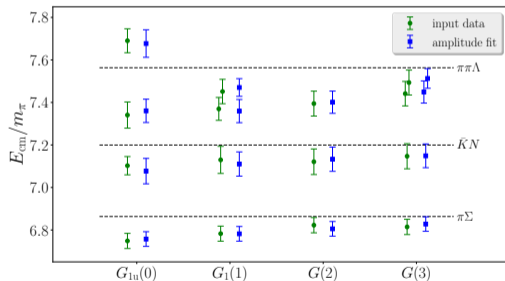
$$\det \left[\tilde{K}^{-1}(E_{\text{cm}}) - B^{\text{P}}(E_{\text{cm}}) \right] = 0 \quad \text{Quantization condition}$$

$$\det \left[\begin{pmatrix} \tilde{K}_{\pi\Sigma \rightarrow \pi\Sigma} & \tilde{K}_{\pi\Sigma \rightarrow \bar{K}N} \\ \tilde{K}_{\bar{K}N \rightarrow \pi\Sigma} & \tilde{K}_{\bar{K}N \rightarrow \bar{K}N} \end{pmatrix} + \begin{pmatrix} F_{\pi\Sigma}^{-1}(E_n, \vec{P}, L) & 0 \\ 0 & F_{\bar{K}N}^{-1}(E_n, \vec{P}, L) \end{pmatrix} \right] = 0$$



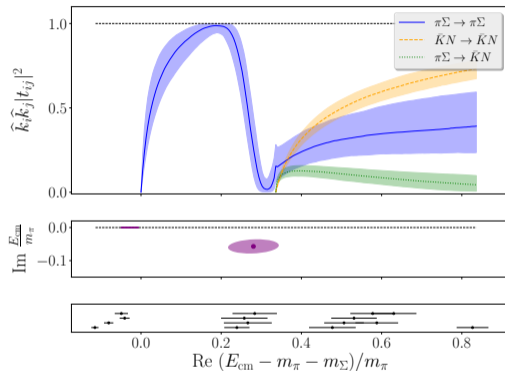
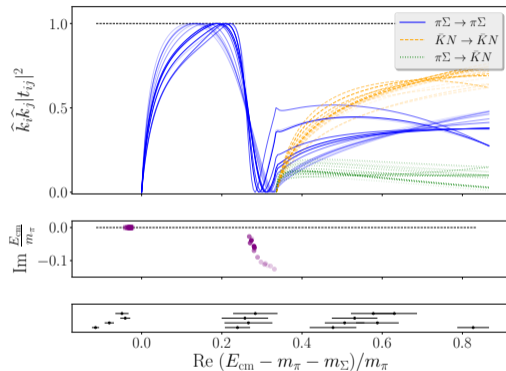
\tilde{K} - matrix
parametrization

$$\begin{cases} \tilde{K}_{ij} = \frac{m_\pi}{E_{\text{cm}}} (A_{ij} + B_{ij} \Delta_{\pi\Sigma}) \\ \tilde{K}_{ij}^{-1} = \frac{E_{\text{cm}}}{m_\pi} (\tilde{A}_{ij} + \tilde{B}_{ij} \Delta_{\pi\Sigma}) \\ \tilde{K} = CFC^{-1} \\ \tilde{K}_{ij} = \hat{C}_{ij}(2E_{\text{cm}} - M_i - M_j) \end{cases}$$



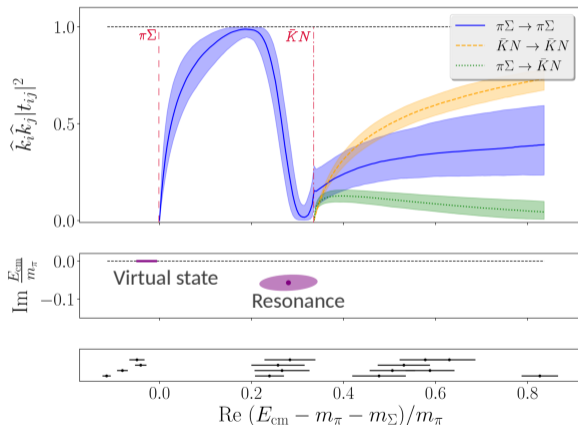
The scattering transition amplitude:

$$t^{-1} = \tilde{K}^{-1} - i\hat{k}$$



(Left) Scattering amplitude results based on different parametrizations

(Right) Preferred parametrization of the scattering amplitude



Virtual bound state

$$E_1 = 1392(9)_{\text{st}}(2)_{\text{md}}(16)_{\text{a}} \text{ MeV}$$

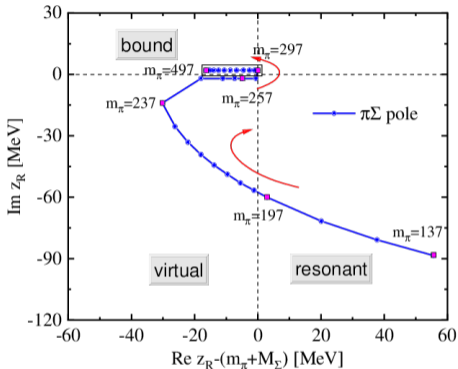
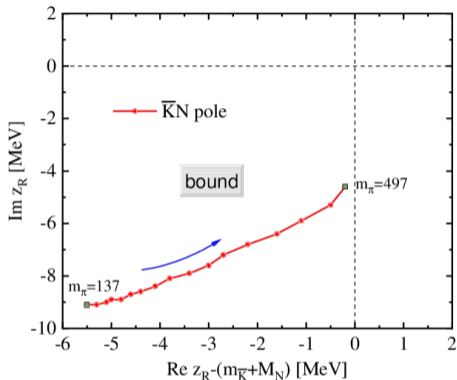
$$\left| \frac{c_{\pi\Sigma}^{(1)}}{c_{\bar{K}N}^{(1)}} \right| = 1.9(4)_{\text{st}}(6)_{\text{md}}$$

Resonance

$$E_2 = [1455(13)_{\text{st}}(2)_{\text{md}}(17)_{\text{a}}$$

$$-i11.5(4.4)_{\text{st}}(4.0)_{\text{md}}(0.1)_{\text{a}}] \text{ MeV}$$

$$\left| \frac{c_{\pi\Sigma}^{(2)}}{c_{\bar{K}N}^{(2)}} \right| = 0.53(9)_{\text{st}}(10)_{\text{md}}$$



Trajectories of the two poles of $\Lambda(1405)$ as functions of the pion mass m_π from 137 MeV to 497 MeV. Critical masses are labeled by solid squares, between which the points are equally spaced. ($z_R = m_R - i\Gamma_R/2$) [Xie et al., PRD 108 (2023) 11]

Table of Contents

- ⊙ About the $\Lambda(1405)$
- ⊙ Lattice QCD
- ⊙ Finite-volume energy spectra
- ⊙ Scattering amplitude analysis
- ⊙ Summary

- First Lattice QCD study of coupled-channel $\pi\Sigma - \bar{K}N$ in the $\Lambda(1405)$ region
- Every parametrization used found two poles in this region
 - ✧ **NOTE:** These parametrizations could accommodate zero, one or two poles
- Our results show qualitative agreement with phenomenological extractions [See PDG, section 83]

Lower Pole: $E_1 = 1392(9)_{\text{stat}}(2)_{\text{model}}(16)_{\text{a}} \text{ MeV}$

Higher Pole: $E_2 = [1455(13)_{\text{stat}}(2)_{\text{model}}(17)_{\text{a}} - i11.5(4.4)_{\text{stat}}(4.0)_{\text{model}}(0.1)_{\text{a}}] \text{ MeV}$

Reference Results: $\text{Re}(E_1) = 1325 - 1380 \text{ MeV}; \quad \text{Re}(E_2) = 1421 - 1434 \text{ MeV}$

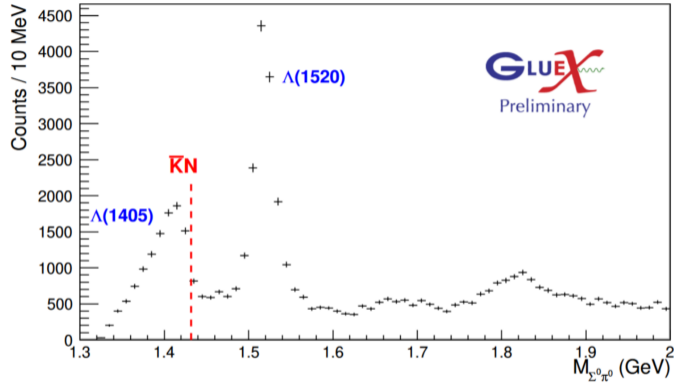
- **Future work:**
 - Explore quark masses dependence of the poles
 - Study lattices with a closer to physical m_π

Thanks



Table of Contents

⦿ Back-up



Wickramaarachchi et al., EPJ Web Conf. 271 (2022) 07005, [e-Print: 2209.06230]

Ensemble **D200** generated by CLS was used. Its properties are:

- Dynamical mass-degenerate u - and d -quarks (heavier than physical), and s -quark (lighter than physical).
- Tree-level improved Lüscher-Weisz gauge action.
- Non-perturbatively $\mathcal{O}(a)$ -improved Wilson fermion action.

The effective mass is calculated as:

$$m_{eff}(t + 1/2) = \ln \left(\frac{C(t)}{C(t+1)} \right)$$

$$\chi^2 = \sum_{t, t'=t_{min}}^{t_{max}} (C(t) - f(t)) \frac{1}{Cov_N(t, t')} (C(t') - f(t'))$$

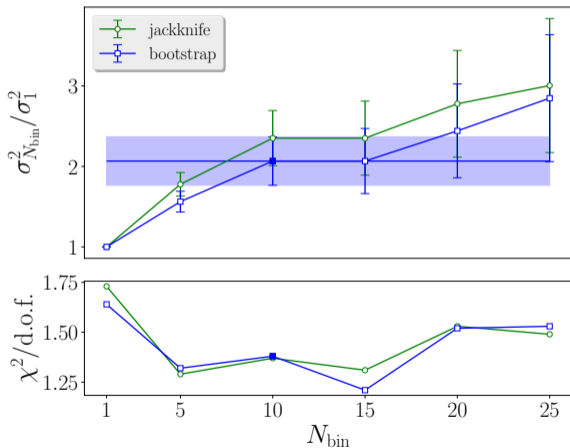
where

$$f(t) = A_i e^{-E_i t}$$

and

$$Cov_N(t, t') = \frac{1}{N-1} \langle (C(t) - \langle C(t) \rangle_N) (C(t') - \langle C(t') \rangle_N) \rangle_N$$

t, t' : lattice time E_i : Energy N : Nr. samples $\langle \dots \rangle_N$: statistical average



(Top) Ratios of variances for fits to m_π versus N_{bin} for jackknife and bootstrap resampling.

(Bottom) Correlated- χ^2 of two-exponential fit to m_π versus N_{bin} . In both panels, the final binning choice is illustrated as a blue solid square.

am_π	0.06533(25)	am_K	0.15602(16)	am_N	0.3143(37)
am_Λ	0.3634(14)	am_Σ	0.3830(19)	am_Ξ	0.41543(96)

Table: Summary of hadron masses in Lattice units.

am_π	~ 200	am_K	~ 487	am_N	~ 980
am_Λ	~ 1120	am_Σ	~ 1194	am_Ξ	~ 1295

Table: Summary of hadron masses in MeV units.

Basically one searches for the zero's of the following equation, using the finite-volume energy spectra as constrain.

$$\det \left[\underbrace{\begin{pmatrix} \tilde{K}_{\pi\Sigma \rightarrow \pi\Sigma} & \tilde{K}_{\pi\Sigma \rightarrow \bar{K}N} \\ \tilde{K}_{\bar{K}N \rightarrow \pi\Sigma} & \tilde{K}_{\bar{K}N \rightarrow \bar{K}N} \end{pmatrix}}_{\text{Multi-channel Matrix}} + \underbrace{\begin{pmatrix} F_{\pi\Sigma}^{-1}(E_n, \vec{P}, L) & 0 \\ 0 & F_{\bar{K}N}^{-1}(E_n, \vec{P}, L) \end{pmatrix}}_{\text{Zeta Function}} \right] = 0$$

One fits with respect to the energy shifts of the non-interacting energies:

$$\Delta E_i = E_{\text{cm}}^{\text{latt}} - E_{\text{cm}}^{\text{free}}$$

Where one minimize correlated χ^2 :

$$\delta_i = \Delta E_{\text{cm},i} - \Delta E_{\text{cm},i}^{\text{QC}}$$

And the preferred fit is based on lowest Akaike Information Criterion:

$$\text{AIC} = \chi^2 - 2n_{\text{dof}}$$

The following quantity is defined proportional to the scattering transition amplitude and to \tilde{K} as:

$$t^{-1} = \tilde{K}^{-1} - i\hat{k}$$

where $\hat{k} = \text{diag}(k_{\pi\Sigma}, k_{\tilde{K}N})$, and

$$k_{\pi\Sigma}^2 = \frac{1}{E_{\text{cm}}^2} \lambda_K(E_{\text{cm}}^2, m_{\pi}^2, m_{\Sigma}^2)$$

$$k_{\tilde{K}}^2 = \frac{1}{E_{\text{cm}}^2} \lambda_K(E_{\text{cm}}^2, m_{\tilde{K}}^2, m_N^2)$$

where λ_K is the Källén function. Which is equivalent to searching for the ∞ 's of

$$t = \frac{1}{E_{\text{cm}} - E_{\text{pole}}} \begin{pmatrix} c_{\pi\Sigma}^2 & c_{\pi\Sigma} c_{\tilde{K}N} \\ c_{\pi\Sigma} c_{\tilde{K}N} & c_{\tilde{K}N}^2 \end{pmatrix} + \dots$$

1. An effective range expansion (ERE) of the form

$$\tilde{K}_{ij} = \frac{m_\pi}{E_{\text{cm}}} \left(A_{ij} + B_{ij} \Delta_{\pi\Sigma}(E_{\text{cm}}) \right). \quad (1)$$

2. A variation of the first parametrization without the factor of m_π/E_{cm} :

$$\tilde{K}_{ij} = \hat{A}_{ij} + \hat{B}_{ij} \Delta_{\pi\Sigma}(E_{\text{cm}}). \quad (2)$$

3. An ERE of \tilde{K}^{-1} of the form

$$\tilde{K}_{ij}^{-1} = \frac{E_{\text{cm}}}{m_\pi} \left(\tilde{A}_{ij} + \tilde{B}_{ij} \Delta_{\pi\Sigma}(E_{\text{cm}}) \right). \quad (3)$$

1. A Blatt-Biedenharn parametrization:

$$\tilde{K} = C F C^{-1}, \quad (4)$$

where

$$C = \begin{pmatrix} \cos \epsilon & \sin \epsilon \\ -\sin \epsilon & \cos \epsilon \end{pmatrix}, \quad (5)$$

$$F = \begin{pmatrix} f_0(E_{\text{cm}}) & 0 \\ 0 & f_1(E_{\text{cm}}) \end{pmatrix}, \quad (6)$$

and

$$f_i(E_{\text{cm}}) = \frac{m_\pi}{E_{\text{cm}}} \frac{a_i + b_i \Delta_{\pi\Sigma}(E_{\text{cm}})}{1 + c_i \Delta_{\pi\Sigma}(E_{\text{cm}})}. \quad (7)$$

2-pole picture

Different CLAS analysis

→ Roca & Oset, PRC **88** (2013) 055206

→ Mai & Meißner, EPJA **51** (2015) 30

BGOOD analysis

→ Schluchin et al., PLB **833** (2022) 137375

ALICE at LHC analysis

→ Acharya et al., EPJC **83** (2023) 340

Preliminary GlueX analysis

→ Wickramaarachchi et al., EPJ **271** (2022) 07005

Chiral approaches

→ Oller & Meißner, PLB **500** (2001) 263

1-pole picture

J-PARC analysis

→ Aikawa et al., PLB **837** (2023) 137637

Simple quark models

→ Isgur & Karl, PRD **18** (1978) 4187

Combined analysis from different experimental data

(does not exclude two-pole picture)

→ Anisovich et al., EPJA **56** (2020) 139

- EPJ: Eur. Phys. Journal
- EPJA: Eur. Phys. Journal A
- EPJC: Eur. Phys. Journal C
- NPA: Nucl. Phys. **A**
- NPB: Nucl. Phys. **B**
- PLB: Phys. Lett. **B**
- PRC: Phys. Rev. **C**
- PRD: Phys. Rev. **D**
- PRL: Phys. Rev. **L**